



Quantitative Identification of Yellow Rust, Powdery Mildew and Fertilizer-Water Stress in Winter Wheat Using *In-Situ* Hyperspectral Data

Qingsong Guan^{1,2}, Wenjiang Huang^{1,*}, Jinling Zhao², Liangyun Liu¹, Dong Liang², Linsheng Huang², Li Wang¹, and Guijun Yang³

¹Key Laboratory of Digital Earth Sciences, Institute of Remote Sensing and Digital Earth, Chinese Academy of Sciences, Beijing 100094, China

²Key Laboratory of Intelligent Computing and Signal Processing, Ministry of Education, Anhui University, Hefei 230039, Anhui, China

³Beijing Agriculture Information Technology Research Center, Beijing 100097, China

(Received: 30 June 2013. Accepted: 12 September 2013)

As the progressive effects of global warming, the yield loss caused by diseases and pests are increasing in winter wheat. It is necessary to distinguish different diseases for guiding variable rate spraying in wheat. Nevertheless, it is very difficult to quantitatively identify different diseases and fertilizer-water stress by specific sensitive bands selected from multi spectral data over a large area. Conversely, hyper spectral data contain more information, and provide the potential for quantitative identification of different stresses. This study focused on identification and distinction of yellow rust, powdery mildew and fertilizer-water stress by canopy spectral reflectance. Fifteen commonly used vegetation indices were selected, and independent *t*-test was done to get sensitivity index for each stress. Finally, a combination index was optimally selected to distinguish the three stresses. The results showed that the integrative index (NDVI-PhRI) combining normalized difference vegetation index (NDVI) and physiological reflectance index (PhRI) could be used to identify powdery mildew and yellow rust (PM-YR). A 2-dimensional spatial coordinate was established based on the NDVI and PhRI derived from hyper spectral data, then the different stress data were displayed in the spatial coordinate and the classification boundary could be used to identify the powdery mildew and yellow rust stress. Similarly, yellow rust and fertilizer-water stress (YR-n0w0) can be distinguished by the combination index (MSR-PhRI) derived from modified simple ratio (MSR) and physiological reflectance index (PhRI); and the combination index (NRI-RVSI) derived from nitrogen reflectance index (NRI) and red-edge vegetation stress index (RVSI) was accurate to identify powdery mildew and fertilizer-water stress (PM-n0w0). For the PM-YR, YR-n0w0 and PM-n0w0 models, their verification accuracies were 83.3%, 88%, 88.75%, and the kappa accuracies were 63.41%, 74.79%, 71.43%, respectively. It indicated that the combination index derived from hyperspectral data could be used to identify the different stresses and provide guides for crop management across a large area.

Keywords: Winter Wheat, Yellow Rust (YR), Powdery Mildew (PM), Fertilizer-Water Stress (n0w0), Canopy Reflectance.

1. INTRODUCTION

Winter wheat (*Triticum aestivum* L.) is one of the most important food grain crops in the world. However, global climate change has already had observable effects on the environment, which has resulted in more stresses than

usual in wheat production. In general, the conventional stresses in winter usually refer to water stress and nitrogen stress, which can cause major yield loss in winter wheat. In recent years, the majority of wheat varieties are less resistant to yellow rust, powdery mildew and other pests and diseases. The crop diseases were inclined to outbreak and cause the rapid spread when environmental conditions

*Corresponding author; E-mail:

were appropriate. Yellow rust and powdery mildew are infectious diseases across a large area, and can cause significant yield loss.¹ To figure out where the stresses are coming from and what they are specifically in wheat plants has led to much concerns on precision agriculture. Thus, it is necessary to quantitatively identify different stresses for agricultural management guides in wheat.

In comparison with traditional methods depending on manual and visual assessment, many advanced techniques have been used for stress detecting and monitoring, including ultrasound technology, nuclear magnetic resonance (NMR), X-ray techniques, multispectral and hyperspectral technology and so on. Each technology has its own advantages in detecting crop stress; however, hyperspectral technology has the more potential for accurately detecting and distinguishing diseases over the large area.²

Some studies have just focused on monitoring yellow rust or powdery mildew of winter wheat using different remote sensing data. The spectral range of optical remote sensing systems mainly relates to ultraviolet (200–400 nm), visible (400–800 nm) and near-infrared (800–2500 nm) bands which were generally used in disease monitoring. The reflectivity in these bands have more direct responses to biochemical state (pigment content, nutrient and moisture content) and physiological state of the plant (structure, morphology).^{3–5} Huang et al.⁶ investigated the relationship between the spectral reflectance and disease severity and screened the diseases sensitive bands. Liu et al.⁷ found that wheat yellow rust is closely related to the 560–670 nm band reflectance and then constructed a measurement model. Graeff et al.⁸ found that the sensitive bands were located in 490, 510, 516, 540, 780, and 1300 nm by analyzing the leaf spectra of wheat infected with powdery mildew and take-all disease, Huang et al.⁶ successfully monitored the wheat disease using photochemical reflectance index (PRI). In terms of stress recognition, Bravo et al.⁹ investigated the application of hyperspectral data in winter wheat for early detection of yellow rust disease. Luo et al.¹⁰ identified yellow rust from the conventional stress via the feature space that was constituted by Normalized difference vegetation index (NDVI) and Physiological reflectance index (PhRI), and the accuracy was more than 70%. Devadas et al.¹¹ attempted to distinguish yellow rust, leaf rust and stem rust by spectral features. As demonstrated by their studies, ARI (Anthocyanin Reflectance Index) can effectively distinguish normal and yellow rust blade, but cannot accurately distinguish leaf rust and stem rust blade, while TCARI (Transformed Chlorophyll Absorption and Reflectance Index) could.

Previous studies showed that the changes in chlorophyll and moisture content were similar for different crops under different stresses, but they were very different for crop management in the field under different stresses. For example, the application of pesticide to water-stressed crops will

lead to crop damage and yield loss. The ref how to identify disease and fertilizer-water stress is very important for precision crop management.

In this study, four different treatments (yellow rust, powdery mildew, fertilizer-water stress and normal) were applied in the experimental field. The sensitive bands for each stress was identified by qualitative analysis, and then the vegetation indices were extracted and the responses to various stresses were analyzed. Finally, the selected combination vegetation indices were used for the quantitative identification and verification of different stresses. This study can provide a theoretical basis for hyper spectral remote sensing applied for quantitative identification of different stresses and guiding the crop management accurately.

2. MATERIALS AND METHODS

2.1. Experimental Design and Field Conditions

The experiments were conducted at Beijing Xiaotangshan Precision Agriculture Experimental Base, located in Changping District, Beijing (40° 10.6' N, 116° 26.3' E) during the 2001–2002 growing season. The average topsoil nutrient status was as follows: organic matter 1.4%, alkali-hydrolysis nitrogen 63.3 mg/kg, and rapidly available potassium 123.4 mg/kg. The experimental field has a length of 200 m and a width of 80 m.

Two wheat cultivars (98–100 and Beinong 10) were used in the disease experiment. The 98–100 is susceptible to yellow rust and Beinong 10 is susceptible to powdery mildew. Yellow rust and powdery mildew were inoculated by spore inoculation according to the National Plant Protection Standard¹² in early April, 2002. Three cultivars used in fertilizer-water stress experiment were 'Jingdong 8', 'Jing 9428' and 'Zhongyou 9507'. The experiment included nine treatments of fertilizer-water stress and one normal processing, and the planting area was 0.3 ha. Nine fertilizer-water stress treatments were as follows: 300 kg·ha⁻¹ nitrogen and 300 m³·ha⁻¹ water; 300 kg·ha⁻¹ nitrogen and 150 m³·ha⁻¹ water; 300 kg·ha⁻¹ nitrogen and no irrigation; 100 kg·ha⁻¹ nitrogen and 300 m³·ha⁻¹ water; 100 kg·ha⁻¹ nitrogen and 150 m³·ha⁻¹ water; 100 kg·ha⁻¹ nitrogen and no irrigation; no fertilization and 300 m³·ha⁻¹ water; no fertilization and 150 m³·ha⁻¹ water; no fertilization and no irrigation. Normal processing was applied with a recommended rate¹³ which received 200 kg·ha⁻¹ nitrogen and 450 m³·ha⁻¹ water. Three cultivars were evenly distributed in each treatment plot.

2.2. Measurements of Canopy Spectra

A high spectral resolution ASD Field Spec Prospectrometer (Analytical Spectral Devices, Boulder, CO, USA) fitted with a 25 degree field of view fore-optic was used to measure *in-situ* canopy spectral reflectance. All canopy spectral measurements were taken from a height of 1.3 m above ground (the height of the wheat is 90 ± 3 cm at

maturity). Spectra were acquired in the 350–2500 nm spectral range at a spectral resolution of 3 nm between 350 nm and 1050 nm and 10 nm between 1050 nm and 2500 nm. A 40 cm × 40 cm BaSO₄ calibration panel was used for calculating the reflectance. All irradiance measurements were recorded as an average of 20 scans at an optimized integration time. The field measurements were made under clear sky conditions between 10:00 and 14:00 (Beijing local time).

3. RESULTS AND ANALYSIS

3.1. Canopy Spectral Features

In order to extract the sensitive bands from different stresses, the *in-situ* canopy spectral reflectance curves of normal treatment (Normal), yellow rust (YR), powdery mildew (PM) and fertilizer-water stress (n0w0) in winter wheat were obtained during three critical growth periods (Figs. 1(a)–(c)).

In comparison with the spectrum of Normal, the spectra of YR, PM and n0w0 had almost the same change trend at different growth stages. The canopy reflectance of Normal wheat was lower in yellow region (550–660 nm) and higher in near infrared region (760–1350 nm) compared to the stressed wheat by yellow rust, powdery mildew and fertilizer-water. The canopy spectral reflectance of stressed wheat was significantly lower than that of the Normal, especially at 760 nm. In general, two moisture absorption valleys (1450 and 1950 nm) also became shallow. The results showed that the spectral features of yellow rust, powdery mildew and fertilizer-water stress were similar and was difficult to identify the different stresses using the wide sensitive bands. Conversely, the hyper spectral curves could separate them and provided the possibility for the identification of different stresses (Fig. 1).

3.2. Vegetation Indices and Responses

The combination vegetation index was used to identify the different stresses. As shown in Table I, fifteen commonly used vegetation indices were selected, which were sensitive to chlorophyll content, canopy architecture or water status of plants. For example, Structural Independent Pigment Index (SIPI) is closely associated with chlorophyll content, and Normalized Difference Vegetation Index (NDVI) and Moisture Stress Index (MSI) are sensitive to canopy architecture and water status of plants, respectively.

The *T*-test was done to each vegetation index for independent samples. (Table II) I indicated that the responses of vegetation indices (VIs) to different stresses were discrepant, and some indices may only respond to a certain stresses.

As shown in Table II, most vegetation indices had significant responses ($p < 0.05$) to yellow rust except for TCARI, SIPI and TVI. Among them, NRI and NPCI reached a very significant level ($p < 0.001$). For the powdery mildew, 10 vegetation indices had significant

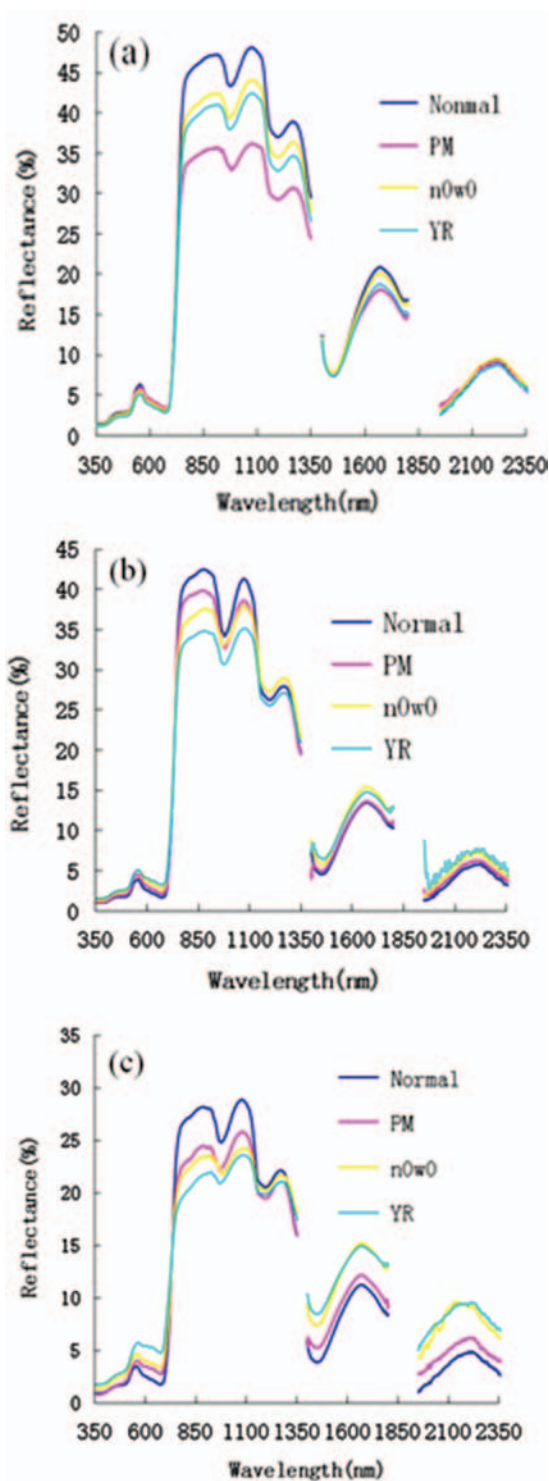


Fig. 1. Comparison of the spectral separability of normal and stressed samples at different growth stages. (a) elongation stage; (b) flowering stage; and (c) filling stage.

responses ($p < 0.05$) Conversely, only 5 vegetation indices had responses to fertilizer-water stress, due to the effect of soil basal fertilizer. According to the analysis results, the combination indices derived from NDVI and PhRI (NDVI-PhRI), MSR and PhRI (MSR-PhRI), NRI and

Table I. Definitions of a set of vegetation indices used in this study.

| Vegetation index | Definition | Description | Literatures |
|------------------|--|--|--|
| MSR | Modified simple ratio | $(R_{800}/R_{670} - 1)/(R_{800}/R_{670} + 1)^{1/2}$ | Chen (1996); Haboudane et al. (2004) ^{14,15} |
| NDVI | Normalized difference vegetation index | $(R_{840} - R_{675})/(R_{840} + R_{675})$ | Rouse et al. (1973) ¹⁶ |
| NRI | Nitrogen reflectance index | $(R_{570} - R_{670})/(R_{570} + R_{670})$ | Filella et al. (1995) ¹⁷ |
| PRI | Photochemical reflectance index | $(R_{570} - R_{531})/(R_{570} + R_{531})$ | Gamon et al., 1992 ¹⁸ |
| TCARI | The transformed chlorophyll absorption and reflectance index | $3 \times [(R_{700} - R_{670}) - 0.2 \times (R_{700} - R_{550}) \times (R_{700}/R_{670})]$ | Haboudane et al. (2002) ¹⁹ |
| SIPI | Structural independent pigment index | $(R_{800} - R_{445})/(R_{800} - R_{680})$ | Peñuelas et al. (1995) ²⁰ |
| PSRI | Plant senescence reflectance index | $(R_{680} - R_{500})/R_{750}$ | Merzlyak et al. (1999) ²¹ |
| PhRI | Physiological reflectance index | $(R_{550} - R_{531})/(R_{550} + R_{531})$ | Gamon et al. (1992) ¹⁸ |
| NPCI | Normalized pigment chlorophyll ratio index | $(R_{680} - R_{430})/(R_{680} + R_{430})$ | Peñuelas et al. (1994) ²² |
| ARI | Anthocyanin reflectance index | $(R_{550})^{-1} - (R_{700})^{-1}$ | Gitelson et al. (2001) ²³ |
| TVI | Triangular vegetation index | $0.5[120(R_{750} - R_{550}) - 200(R_{670} - R_{550})]$ | Broge and Leblanc (2000) ²⁴ ; Haboudane et al. (2004) ¹⁵ |
| DSWI | Disease water stress index | $(R_{802} + R_{547})/(R_{1657} + R_{682})$ | Galvão et al. (2005) ²⁵ |
| MSI | Moisture stress index | R_{1600}/R_{819} | Hunt and Rock (1989); Ceccato et al. (2002) ^{26,27} |
| RVSI | Red-edge vegetation stress index | $[(R_{712} + R_{752})/2] - R_{732}$ | Merton and Huntington (1999) ²⁸ |
| MCARI | Modified chlorophyll absorption in reflectance index | $(R_{701} - R_{671}) - 0.2(R_{701} - R_{549})/(R_{701}/R_{671})$ | Daughtry et al. (2000) ²⁹ |

RVSI (NRI-RVSI) were used to identify powdery mildew and yellow rust (PM-YR), yellow rust and fertilizer-water stress (YR-n0w0), and powdery mildew and fertilizer-water stress (PM-n0w0), respectively.

3.3. Quantitative Identification of Different Stresses on Winter Wheat

3.3.1. Prediction Models Based on 2-Dimensional Feature Space

The prediction models were established for distinguishing the PM-YR, YR-n0w0 and PM-n0w0. 20 PM samples

Table II. Independent *t*-tests for four different stresses.

| Index | Stress | | |
|-------|--------------------|--------------------|--------------------|
| | YR | PM | n0w0 |
| MSR | 0.003 ^b | 0.069 | 0.064 |
| NDVI | 0.008 ^b | 0.019 ^a | 0.056 |
| NRI | 0.000 ^c | 0.046 ^a | 0.052 |
| PRI | 0.004 ^b | 0.332 | 0.401 |
| TCARI | 0.329 | 0.017 ^a | 0.884 |
| SIPI | 0.058 | 0.006 ^b | 0.050 |
| PSRI | 0.005 ^b | 0.004 ^b | 0.037 ^a |
| PhRI | 0.041 ^a | 0.325 | 0.578 |
| NPCI | 0.000 ^c | 0.006 ^b | 0.060 |
| ARI | 0.001 ^b | 0.047 ^a | 0.034 ^a |
| TVI | 0.844 | 0.831 | 0.604 |
| DSWI | 0.013 ^a | 0.125 | 0.029 ^a |
| MSI | 0.027 ^a | 0.039 ^a | 0.015 ^a |
| RVSI | 0.005 ^b | 0.005 ^b | 0.017 ^a |
| MCARI | 0.014 ^a | 0.003 ^b | 0.218 |

Notes: ^aMean difference is significant at 0.950 confidence level; ^bMean difference is significant at 0.990 confidence level; ^cMean difference is significant at 0.999 confidence level.

and 20 YR samples were used for the PM-YR, and the 2-dimensional feature space coordinate was established with NDVI as the abscissa and PhRI as the vertical axis (Fig. 2(a)). In the 2-dimensional feature space, the samples were distributed in different regions. According to the distribution of samples, the discriminant curve of stress samples could be established. The quadratic equation ($\text{PhRI} = 0.073 \text{NDVI}^2 - 0.022 \text{NDVI} + 0.05$) was obtained by fitting the stress samples near the classification border. If the observation point was above the discriminant curve, we believed that it was the YR sample, otherwise, it was the PM sample. The model accuracy reached 82.5% using the 40 modeling samples (Table III). The 2-dimensional feature space of YR-n0w0 and PM-n0w0 were shown in Figures 2(b) and (c). For the YR-n0w0 and PM-n0w0, the quadratic equations were $\text{PhRI} = 0.0078 \text{MSR}^2 - 0.0223 \text{MSR} + 0.0773$ and $\text{RVSI} = 3.395 \text{NRI}^2 + 1.984 \text{NRI} - 1.382$, and the accuracies were 87.5% and 82.5%, respectively (Tables IV and V).

3.3.2. Verification

Another 20 PM samples, 40 YR samples and 60 n0w0 samples, except for building up the models, were used to test the accuracies of prediction models in this study (Fig. 3). Classification prediction of verification samples were assessed using the overall accuracy and Kappa coefficient, and the error matrices were calculated (Tables VI–VIII). The results showed that the overall accuracies of PM-YR, YR-n0w0 and PM-n0w0 were 83.3%, 88%, 88.75%, and Kappa coefficients were 63.41%, 74.79%, 71.43%. Therefore, the proposed method can be used to identify the stress samples.

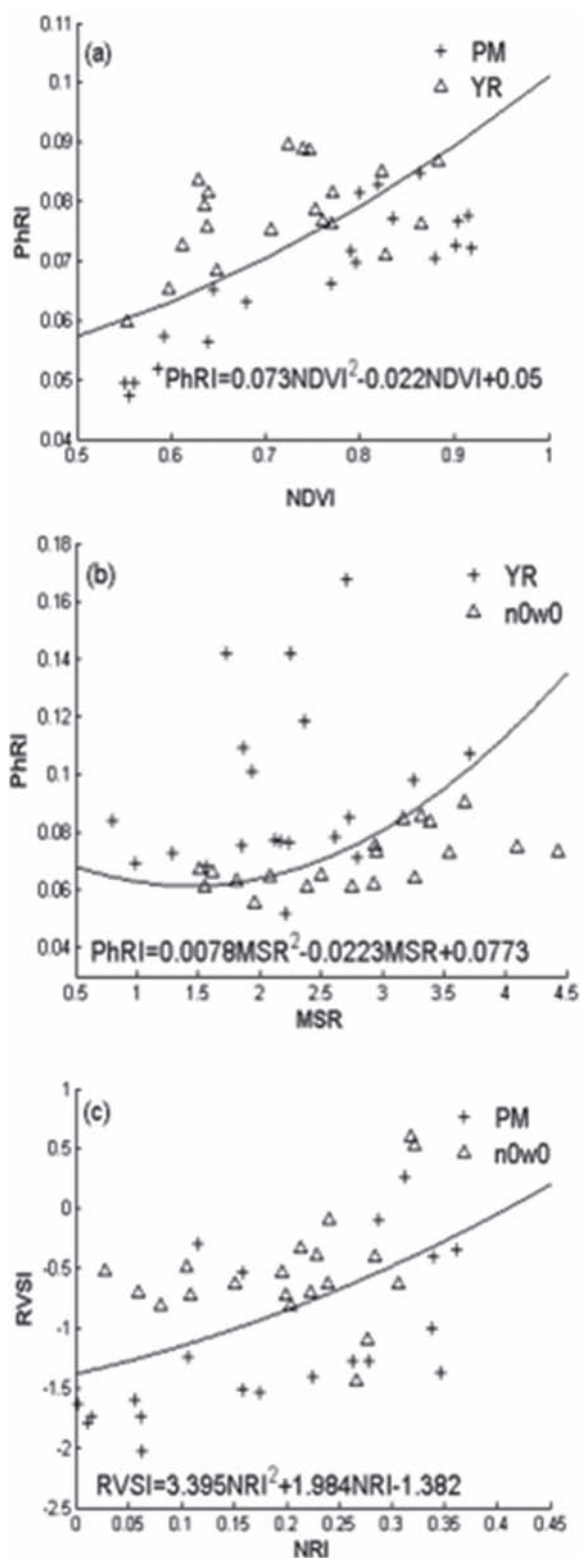


Fig. 2. Quantitative identification and prediction models for different stresses. (a) PM-YR; (b) YR-n0w0; and (c) PM-n0w0.

4. DISCUSSION

It is important to distinguish the different stresses in the farmland management. However, it is difficult to achieve

Table III. Identification accuracy of the PM-YR model.

| Stress | Sample points | Correct points | Accuracy (%) |
|--------|---------------|----------------|--------------|
| PM | 20 | 18 | 90 |
| YR | 20 | 15 | 75 |
| Total | 40 | 33 | 82.5 |

Table IV. Identification accuracies of the YR-n0w0 model.

| Stress | Sample points | Correct points | Accuracy (%) |
|--------|---------------|----------------|--------------|
| YR | 20 | 18 | 90 |
| n0w0 | 20 | 17 | 85 |
| Total | 40 | 35 | 87.5 |

Table V. Identification accuracies of the PM-n0w0 model.

| Stress | Sample points | Correct points | Accuracy (%) |
|--------|---------------|----------------|--------------|
| PM | 20 | 16 | 80 |
| n0w0 | 20 | 17 | 85 |
| Total | 40 | 33 | 82.5 |

Table VI. The error matrices of verification samples (PM-YR).

| | PM | YR | Total |
|-------|----|----|-------|
| PM | 16 | 4 | 20 |
| YR | 6 | 34 | 40 |
| Total | 22 | 38 | 60 |

Kappa coefficient = 0.6341.

Table VII. The error matrices of verification samples (YR-n0w0).

| | YR | n0w0 | Total |
|-------|----|------|-------|
| YR | 33 | 7 | 40 |
| n0w0 | 5 | 55 | 60 |
| Total | 38 | 62 | 100 |

Note: Kappa coefficient = 0.7479.

such a goal without enough prior knowledge using current methods. Hyper spectral imaging can potentially and rapidly detect stresses or diseases for crops over large areas.² Moshou et al.³⁰ utilized spectral images from 460 to 900 nm to successfully detect yellow rust in wheat.

However, this study was performed under almost the same ecological conditions, and it cannot be applied directly to different ecological conditions. Studies on how environmental conditions influence on different stresses

Table VIII. The error matrices of verification samples (PM-n0w0).

| | PM | n0w0 | Total |
|-------|----|------|-------|
| PM | 17 | 3 | 20 |
| n0w0 | 6 | 54 | 60 |
| Total | 23 | 57 | 80 |

Kappa coefficient = 0.7143.

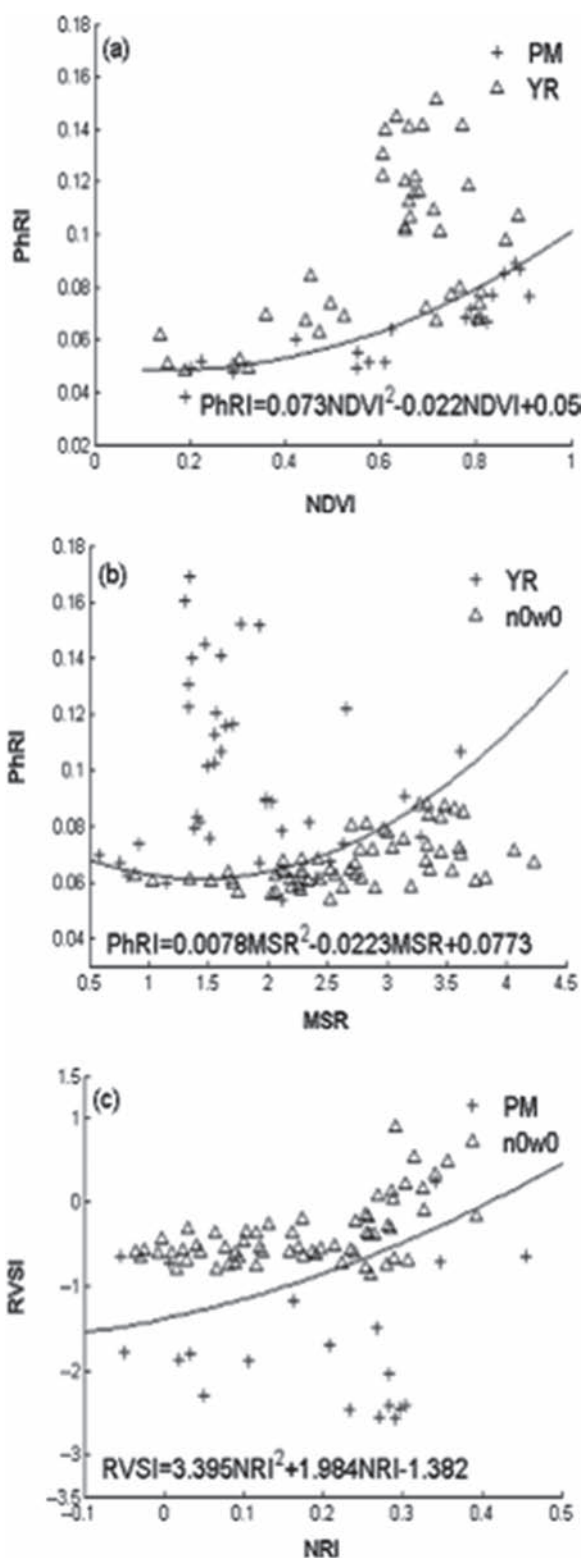


Fig. 3. Validation results of three prediction models. (a) PM-YR; (b) YR-n0w0; and (c) PM-n0w0.

should be carried out later. Moreover, spectral features used in this study were limited, which may not reflect the essential characteristics of the stress. More spectral features should be considered for further studies.

5. CONCLUSION

Nutrient stress, including water and nitrogen fertilizer excess and deficiency, is the common stress type of farmland management. Responses to diseases and nutrient stress in crops have good consistency, and it remains difficult and challenging for remote sensing technologies to identify crop diseases and nutrient stresses.³¹

In this study, we compared the spectral curves of different stresses and calculated the responses of 15 commonly used vegetation indices using independent samples *T*-test method. Finally, NDVI-PhRI, MSR-PhRI and NRI-RVSI were used to identify powdery mildew and yellow rust (PM-YR), yellow rust and fertilizer-water stress (YR-n0w0), and powdery mildew and fertilizer-water stress (PM-n0w0), respectively. The verification results showed that the overall accuracies were 83.3%, 88%, 88.75%, and Kappa accuracies were 63.41%, 74.79%, 71.43%, respectively. Therefore, the quantitative identification models can be used to predict the stress types of samples. The prediction models are established during three critical growth periods (elongation stage, flowering stage, and filling stage) of winter wheat and have good practicability.

Acknowledgments: This work was subsidized by Hundred Talent Program of the Chinese Academy of Sciences of Wenjiang Huang, National Natural Science Foundation of China (41271412, 41071276), the Major state Basic Research Development Program of China (2010CB950603), and the Special Support by China Postdoctoral Science Foundation (2013T60080). The authors are grateful to Mr. Weiguo Li, Mrs. Hong Chang and Zhihong Ma for data collection.

References and Notes

1. R. P. Singh, J. Huerta-Espino, and A. P. Roelfs, The wheat rusts, edited by B. C. Curtis, S. Rajaram, and H. G. Macherson, Bread Wheat-Improvement and Production, Plant Production and Protection Series, Food and Agriculture Organisation of the United Nations, Rome, available: http://www.fao.org/documents/show_cdr.asp (accessed 30 October 2008) (2002), Vol. 30.
2. S. Sankaran, A. Mishra, R. Ehsani, and C. Davis, *Computers and Electronics in Agriculture* 72, 1 (2010).
3. B. Lorenzen and A. Jensen, *Remote Sensing of Environment* 27, 201 (1989).
4. T. Kobayashi, E. Kanda, and K. Kitada, *The American Phytopathological Society* 91, 316 (2001).
5. W. J. Huang, Z. Niu, J. H. Wang, L. Y. Liu, C. J. Zhao, and Q. Liu, *IEEE Transactions on Geoscience and Remote Sensing* 44, 3601 (2006).
6. W. J. Huang, W. L. David, Z. Niu, Y. J. Zhang, L. Y. Liu, and J. H. Wang, *Precision Agriculture* 8, 187 (2007).
7. M. Y. Huang, W. J. Huang, L. Y. Liu, Y. D. Huang, J. H. Wang, C. J. Zhao, and A. M. Wan, *Transactions of the Chinese Society of Agricultural Engineering* 201, 76 (2004).
8. S. Graeff, J. Link, and W. Claupein, *Central European Journal of Biology* 1, 275 (2006).
9. C. Bravo, D. Moshou, J. West, A. McCartney, and H. Ramon, *Biosystems Engineering* 84, 137 (2003).

10. J. H. Luo, W. J. Huang, C. L. Wei, M. Y. Huang, Y. H. Chen, and J. H. Wang, *Journal of Natural Disasters* 17, 115 (2008).
11. R. Devadas, D. W. Lamb, S. Simpfendorfer, and D. Backhouse, *Precision Agriculture* 10, 459 (2009).
12. G. B. Li, S. M. Zeng, and Z. Q. Li, *Integrated Management of Wheat Pests*, Press of Agriculture Science and Technology of China, Beijing (1989), pp. 185–186.
13. Z. J. Wang, J. H. Wang, L. Y. Liu, W. J. Huang, C. J. Zhao, and C. Z. Wang, *Field Crops Research* 90, 311 (2004).
14. J. M. Chen, *Canadian Journal of Remote Sensing* 22, 229 (1996).
15. D. Haboudane, J. R. Miller, E. Pattery, P. J. Zarco-Tejad, and I. B. Strachan, *Remote Sensing of Environment* 90, 337 (2004).
16. J. W. Rouse, R. H. Haas, J. A. Schell, and D. W. Deering, *Monitoring vegetation systems in the Great Plains with ERTS. Proc. Third ERTS Symposium* (1973), Vol. 1, p. 48.
17. I. Filella, L. Serrano, J. Serra, and J. Penuelas, *Crop Science* 35, 1400 (1995).
18. J. A. Gamon, J. Penuelas, and C. B. Field, *Remote Sensing of Environment* 41, 35 (1992).
19. D. Haboudane, J. R. Miller, N. Tremblay, P. J. Zarco-Tejada, and L. Dextraze, *Remote Sensing of Environment* 81, 416 (2002).
20. J. Peñuelas, F. Baret, and I. Filella, *Photosynthetica* 31, 221 (1995).
21. M. N. Merzlyak, A. A. Gitelson, O. B. Chivkunova, and V. Y. Rakitin, *Physiol. Plantarum* 106, 135 (1999).
22. J. Peñuelas, J. A. Gamon, A. L. Fredeen, J. Merino, and C. B. Field, *Remote Sensing of Environment* 48, 135 (1994).
23. A. A. Gitelson, M. N. Merzlyak, and O. B. Chivkunova, *Photochem. Photobiol.* 74, 38 (2001).
24. N. H. Broge and E. Leblanc, *Remote Sensing of Environment* 76, 156 (2000).
25. L. S. Galvão, A. R. Formaggio, and D. A. Tisot, *Remote Sensing of Environment* 94, 523 (2005).
26. E. R. Hunt and B. N. Rock, *Remote Sensing of Environment* 30, 43 (1989).
27. P. Ceccato, N. Gobron, S. Flasse, B. Pinty, and S. Tarantola, *Remote Sensing of Environment* 82, 188 (2002).
28. R. Merton and J. Huntington, *Summaries of the Eight JPL Airborne Earth Science Workshop*, JPL Publication, Pasadena, CA (1999), pp. 299–307.
29. C. S. Daughtry, C. L. Walthall, M. S. Kim, E. B. de Colstoun, and J. E. McMurtrey, *Remote Sensing of Environment* 74, 229 (2000).
30. D. Moshou, C. Bravo, J. West, S. Wahlen, A. McCartney, and H. Ramon, *Computers and Electronics in Agriculture* 44, 173 (2004).
31. J. S. West, C. Bravo, R. Oberti, D. Lemaire, D. Moshou, and H. A. McCartney, *Annual Review of Phytopathology* 41, 593 (2003).